Feature Article

Toughening by nanostructure

Lorena Ruiz-Pérez, Gareth J. Royston, J. Patrick A. Fairclough, Anthony J. Ryan*

Department of Chemistry, University of Sheffield, Brook Hill, Sheffield S3 7HF, United Kingdom

ABSTRACT

Block copolymer modified epoxy resins have generated significant interest since it was demonstrated that the combination could lead to nanostructured thermosets through self-assembly. Over moderate to high polymer concentration the system behaves as expected for a block copolymer in a solvent selective for one block. Two types of copolymers have been studied: non-reactive and reactive modifiers. Morphologies such as copolymer vesicle and spherical/wormlike micelles can be formed under the appropriate conditions. The enhancement of the modified thermosets' mechanical properties depends on the morphology adopted by the polymers. Besides improving mechanical properties, the morphology was found to also have an effect on the glass transition in the studied systems. In this review we collect the available data on the block copolymers used to fabricate nanostructured epoxy resins and critically appraise the properties reported.

1. Introduction

Hundreds of thousands of tonnes of epoxy resins and their associated hardeners are produced globally each year. Although they are familiar to many as structural adhesives, only a small part of their total production is destined for that purpose. The major fraction will find use in surface coatings, electrical potting and insulation, and as the matrix in fibre reinforced composites, amongst other applications [1,2]. The cured resins often have high service temperatures and are extremely hard wearing. However, these products also tend to be rather brittle due to their high cross-link density and are therefore prone to fracture. In recent years, a considerable amount of work has been undertaken in an attempt to enhance the toughness of these materials. These studies have established that the incorporation of a second phase such as rubber particles, thermoplastic particles or mineral fillers can improve both stiffness and toughness in polymer composites [3,4].

The inclusion of a second phase offers the opportunity to modify the thermal characteristics of epoxy resins such as increasing thermal conductivity or reducing the coefficient of thermal expansion [1]. In addition, the use of metallic fillers can increase the level of electrical conductivity significantly [5].

Traditionally, epoxy-based thermosets have been reinforced with micron-sized fillers or inclusions. The development of

processing techniques over the past twenty years has allowed the size of inclusions to approach the nanoscale. In this fashion, nanosized inclusions are defined as those that have at least one dimension in the range 1–100 nm. In most cases, the efficiency of reinforcing fillers in composites is inversely proportional to the size and directly proportional to the filler surface area to volume ratio [4]. Experiments have shown that compared to microparticles, nanoparticles confer some unique features to polymer composites.

One of these features relates to the interfacial area between the matrix and the filler. Such region a has different properties to the bulk matrix due to polymer–particle interactions. Studies in thin polymer films showed that for classical filled composites (i.e. microsized inclusions) the interfacial region extends into the bulk matrix circa from one to four times the radius of gyration R_g of the matrix [6–8]. In the nano-filled composite scenario, due to the large number density of particles per volume (typically 10^6–10^8 particles/μm^3), the distance between particles (typically 10–50 nm at 1–8 vol% inclusion) is comparable to the size of the interfacial region [9]. Hence, the interfacial region's volume fraction is significantly augmented when compared to the bulk matrix. Such an effect promotes stress transfer from matrix to nanoparticles leading to increased strength and stiffness of the composite [10].

One can certainly speak of 'interface-dominated' materials in this case since such increased interfacial area plays a major role in the composite properties [11]. Different experiments have demonstrated that nanoparticles can significantly improve the Young's modulus of polymers when compared to microparticles

[12,13]. In this way, particle size has a major effect on polymer toughening. It has been shown that the optimum loading of glass beads in an epoxy matrix decreased with decreasing particle size at the microscale [14]. Also, for a given volume fraction of rubber particles, the smaller the particles the higher the toughness achieved in the composite [15]. Furthermore, in some glass filled systems there is a critical volume fraction at which aggregation occurs and the modulus decreases [16–20]. The necessary loadings of nanofillers in polymer matrices are usually lower than those of their microfillers' counterparts (typically 10–40 vol% for micro-fillers) [11]. Consequently, this lower loading confers nano-filled matrices an enormous advantage when compared to microfilled ones. Besides, many characteristic properties of unmodified polymers such as light weight, transparency, ductility and good processability will be preserved after modifier addition [4].

For the reasons mentioned above the synthesis and applications of polymer nanocomposites (PNC) have become important fields of nanomaterial science, in both industrial and academic research over the past ten years [9,11,21–23]. Two major classes can be derived from the broad range of additives used for PNC modification, soft organic and rigid inorganic particles. In the case of soft fillers nanostructural features such as volume fraction, particle shape, particle-size distribution and internal structure are often interrelated and so it is complex to change one feature independently of the other [24].

In this review we focus our attention on block copolymers as the additives to produce nanostructured inclusions in thermosets. Block copolymers have been the subject of much research over the last three decades, largely due to the interesting behaviour of amphiphilic species [25–31]. In these polymeric systems the blocks show differing affinity towards a potential solvent and, frequently, a tendency to avoid mixing of dissimilar blocks with one another. Such effects lead to the blocks arranging themselves into well-ordered structures with feature sizes determined by the lengths of the blocks – typically on the scale of nanometres [32]. This is the main advantage of block copolymers when compared to homopolymers or random copolymers that form macrophase[1]-separated structures.

The formation of nanostructured systems in cured blends of epoxy resin and diblock copolymer was first reported by Hillmyer et al. in 1997 [33]. Block copolymers had previously been investigated as epoxy toughening agents, however, no nanoscale structure was observed [34]. Since that initial report, a number of research groups have carried out further investigations into a range of epoxy/block copolymer blend systems. The results suggest significant potential for block copolymers in epoxy resins, both as toughening agents for epoxy resins and as templating agents for nanostructured materials. The systems studied to date are summarized in Tables 1–3. A comprehensive evaluation of the morphology and behaviour of reactive and non-reactive block copolymers in thermosets is presented here. Subsequently, the enhancement of mechanical properties dependent on block copolymer morphology will be reviewed. Along with toughening, we discuss other important parameters to consider in PNC such as filler/matrix adhesion and the change in the glass transition temperature that usually follows modification of thermosets.

---

[1] The terms *microphase* and *macrophase* separation are used here in the conventional senses. Microphase separation leads to nanostructured systems with dimensions determined by the size of the individual blocks. The phase boundaries will coincide (approximately) with the inter-block interfaces in the block copolymer. In macrophase separation, separation occurs by nucleation and growth or spinodal decomposition on larger length scales. It is worth noting that the usage of these and similar terms varies between researchers in this field, e.g. the term *microseparated* may be used to describe phase separation on the micron scale.

Table 1
A summary of epoxy-block copolymer blend systems investigated to date

Polymer	Abbreviation	Epoxy + hardener system	References
Poly(ethyleneoxide)-*b*-poly(propylene oxide)	PEO–PPO	BADGE + MDA	[35,36]
Poly(ethylene oxide)-*b*-poly-(butylene oxide)	PEO–PBO	BADGE + PN	[37]
Poly(ethylene oxide)-*b*-poly-(ethyl ethylene)	PEO–PEE	BADGE + PA	[33]
		BADGE + MDA	[38]
Poly(ethyleneoxide)-*b*-poly-(ethylene-*alt*-propylene)	PEO–PEP	BADGE + PA	[33]
		BADGE + MDA	[38,39]
		BADGE + PN	[40]
Poly(ethyleneoxide)-*b*-poly(propylene oxide)-*b*-poly(ethylene oxide)	PEO–PPO–PEO	BADGE + MDA	[36,41–46]
Poly(methylacrylate-*co*-glycidyl methacrylate)-*b*-polyisoprene	P(MA-*co*-GMA)–PI	PN + MDA	[47]
		BADGE + MDA	[48]
Polybutadiene-*b*-poly(epoxy-1,4-isoprene-*ran*-1,4-isoprene)	PB–ePI	BADGE + MDA	[48]
Polystyrene-*b*-polybutadiene	PS–PB	PPGDGE + MDA	[49]
	Star block copolymer	BADGE + MCDEA/DDS	[50,51]
Poly(ethylene oxide)-*b*-polyisoprene	PEO–PI	BADGE + MDA	[39,52]
Poly(ethylene oxide)-*b*-polybutadiene	PEO–PB	BADGE + MDA	[52]
(Epoxidised polyisoprene)-*b*-polybutadiene	ePI–PB	BADGE + MDA	[52]
Poly(methylacrylate-*co*-glycidyl methacrylate)-*b*-poly(2-ethylhexyl methacrylate)	P(MA-*co*-GMA)–PEHMA	BADGE + MDA	[52]
		BADGE (±Br) + PN	[40]
Polystyrene-*b*-polybutadiene-*b*-poly(methyl methacrylate)	SMB	BADGE + MCDEA/DDS	[53,54]
Poly(2-vinylpyridine)-*b*-polyisoprene	P2VP–PI	PN + HMTA	[55,56]
Poly(ethylene oxide)-*b*-poly(ethylene)	PEO–PE	BADGE + MDA	[57]
Poly(ethylene oxide)-*b*-polystyrene	PEO–PS	BADGE + MOCA	[58]
Poly(ε-caprolactone)-*b*-polybutadiene–poly(ε-caprolactone)	PCL–PB–PCL	BADGE + MOCA	[59]
Poly(methyl methacrylate)-*b*-polystyrene	PMMA–PS	BADGE + MXDA	[60]
		BADGE only	[61]
Poly(methyl methacrylate)-*b*-polybutadiene	PMMA–PB	BADGE only	[61]
Polystyrene-*b*-polybutadiene-*b*-poly(methyl methacrylate)-*b*-poly(glycidyl methacrylate)	SMBG	BADGE + MCDEA	[62]
Polystyrene-*b*-polybutadiene-*b*-poly(methyl methacrylate)-*stat*-(methacrylic acid)	SMBA	BADGE + DDS/MCDEA/MDA	[63]

Details of resins and curing agents are given in Table 2. Structures of polymer blocks are given in Table 3.

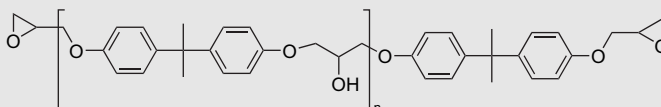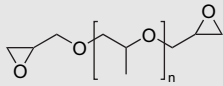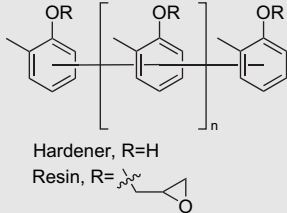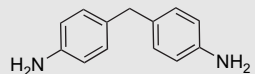## 2. Nanostructured block copolymer – epoxy thermosets: a brief review
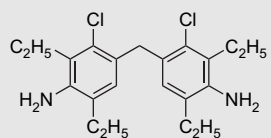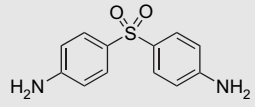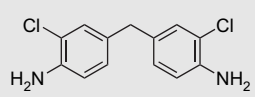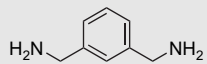
2.1. Non-reactive block copolymers

2.1.1. Studies of morphology and kinetics

In their initial work [33] Hillmyer et al. demonstrated the formation of hexagonally packed cylinders with diameters on the order of tens of nanometres. The epoxy system was bisphenol-A diglycidyl ether (BADGE) + phthalic anhydride (PA). Samples containing both poly(ethylene oxide)-*b*-poly(ethylene-*alt*-propylene) PEO–PEP (36 wt.% diblock in epoxy, $\phi_{PEO}{}^2 = 0.52$) and poly(ethylene oxide)-*b*-poly(ethyl ethylene) PEO–PEE (25 wt.% diblock, $\phi_{PEO} = 0.39$) were analyzed. Cylinders with a core–shell

---

[2] ϕ_{PEO} is the volume fraction of PEO in the diblock.

Table 2
Epoxy resins and curing agents

Name	Abbreviation	Structure
Bisphenol-A diglycidyl ether	BADGE	
Poly(propylene glycol) diglycidyl ether	PPGDGE	
Phenol novolac	PN	Hardener, R=H, Resin, R=
Methylene dianiline	MDA	
4,4′-Methylenebis-(3-chloro-2,6-diethylaniline)	MCDEA	
4,4′-Diaminiodiphenyl sulfone	DDS	
4,4′-Methylenebis-(2-chloroaniline)	MOCA	
m-Xylenediamine	MXDA	

morphology consisting of a non-polar core surrounded by a corona of PEO were observed as shown in Fig. 1.

In subsequent work [38] the same group carried out a comprehensive analysis involving various weight fractions of a PEO–PEP diblock ($\phi_{PEO} = 0.51$, $M_n = 2700$ g/mol) in a system cured with aromatic amine. A phase diagram similar to that predicted by self-consistent field theory [64] for a mixture of diblock with PEO homopolymers was obtained.

An increase in d-spacing was observed as epoxy molecular weight was increased by reaction. These results were determined to be consistent with swelling (or 'wetting') of the PEO block by epoxy resin. The connectivity of the PEO–PEP blocks and the requirements to maintain constant density and minimize chain stretching, lead to augmented interfacial curvature as the concentration of resin is increased. Fig. 2 shows the phase diagram obtained. Examination of the data showing d-spacing against cure time indicates that swelling continues to occur long after the gel-point. This was attributed to the fact that the gel-point is a property of the bulk sample and does not necessarily coincide with the restriction of local mobility on the nanometre scale.

Time resolved small angle X-ray scattering (SAXS) studies performed during curing indicate that for some compositions, order–order phase transitions occur as the epoxy cross-links. An example is shown in Fig. 3 wherein a 69 wt% blend of the PEO–PEP diblock in epoxy is shown to undergo a transition from gyroid to lamellar structure as the reaction progresses. To explain this behaviour, it is suggested that the, initially epoxy miscible, PEO block is expelled from the resin as curing progresses. This expulsion leads to a 'drying' or deswelling of the PEO block, leading to a subsequent reduction in interfacial curvature. Consequently, as long as curing has not progressed so far as to kinetically inhibit the phase transition, a morphology with reduced interfacial curvature will be adopted.

2.1.1.1. Studies with PEO–PPO–PEO triblocks. A number of investigations have been performed using PEO–PPO–PEO triblock copolymers, which are commercially available under the 'Pluronic' trade name. Mijovic et al. [36] examined blends of MDA cured BADGE with a PEO–PPO diblock ($M_n = 12\,000$ g mol^{-1}, 70 wt% PEO) and a PEO–PPO–PEO triblock ($M_n = 4400$ g mol^{-1}, 30 wt% PEO).

Table 3
Block structures of some of the copolymers which have been investigated

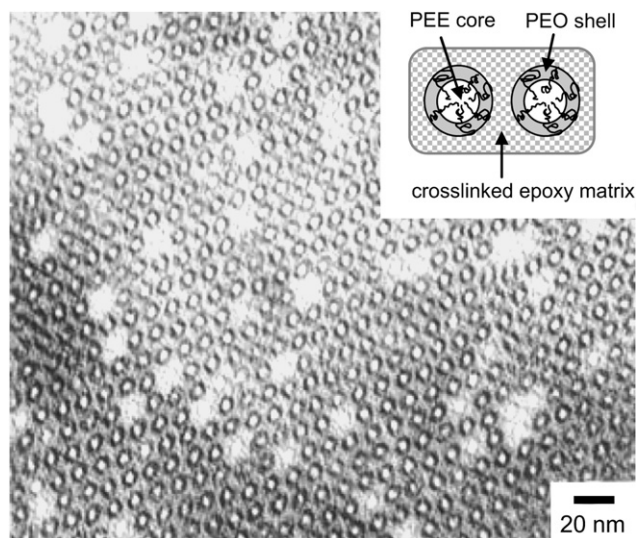| Name	Abbreviation	Structure
Poly(ethylene oxide)	PEO	
Poly(propylene oxide)	PPO	
Poly(butylene oxide)	PBO	
Poly(ethyl ethylene)	PEE	
Poly(ethylene-*alt*-propylene)	PEP	
Polyisoprene	PI	
Poly(1,2-butadiene)	PB	
Polystyrene	PS	
Polyethylene	PE	
Poly(methyl methacrylate)	PMMA	
Poly(ε-caprolactone)	PCL	
Poly(2-vinylpyridine)	P2VP	
Poly(epoxy-1,4-isoprene)	ePI	
Poly(methyl acrylate-*co*-glycidyl methacrylate)	P(MA-*co*-GMA)	

Fig. 1. TEM image showing cylinders of PEO–PEE (25 wt.% $PEO_{36}PEE_{39}$) in an epoxy matrix. The core–shell morphology is clearly visible [33]. Reproduced by permission of the American Chemical Society.

Reaction induced macrophase separation was observed on two different length scales (1 μm and 50 μm) in the triblock system. No visible phase separation occurred in the diblock system. The difference in solubility between the two block copolymers is most likely due to the difference in PEO content.

Guo et al. [41] examined blends of two PEO–PPO–PEO triblocks (30 wt% PEO, $M_n = 5800$ g mol^{-1} and 80 wt% PEO, $M_n = 8400$ g mol^{-1}) in MDA cured BADGE. Microphase separation was observed in all blends from 10% to 50% triblock for both copolymers. This contrasts with the macrophase separation observed with the 30 wt% PEO triblock above. Whether reaction induced phase separation occurs is determined by two factors. These are competition between curing speed – gelation occurs more rapidly at high temperatures – and mobility – viscosity at a given extent of cure will be lower at higher temperatures, reducing kinetic barriers to phase separation. Mijovic et al. cured their blends at 120 °C whereas Guo et al. used an initial cure temperature of 80 °C followed by 150 °C and 175 °C post-cures. This suggests that, at least for this copolymer, the probability of macrophase separation is determined by kinetic factors.

Transmission electron microscopy (TEM) and atomic force measurement (AFM) studies of the cured samples indicated that both block copolymers form structures on the nanometre scale by microphase separation of PPO domains from an epoxy/PEO matrix. In both cases, spherical micelles were formed at low copolymer concentrations (10%). As concentration was increased, PPO domains merged to form, first wormlike micelles and then bicontinuous structures. At 20 wt% block copolymer both systems show hierarchical nanostructures in AFM phase images. Spherical micelles of diameter ∼10 nm are dispersed throughout the resin phase which is composed of harder, epoxy-rich, and softer, copolymer-rich, regions on the 100 nm scale. An example is shown in Fig. 4.

Larrañaga et al. have published a number of papers dealing with the kinetics, nanostructure and mechanical properties of a number of PEO–PPO–PEO/BADGE + MDA systems [42–45].

Curing kinetics of the epoxy system were investigated with increasing amounts of block copolymer additive [44] and with differing volume fractions of PEO in the copolymer [42]. Results from isothermal differential scanning calorimetry (DSC) experiments were fitted to a kinetic model. It was shown that PEO slows the reaction both by acting as a diluent and by interfering with the
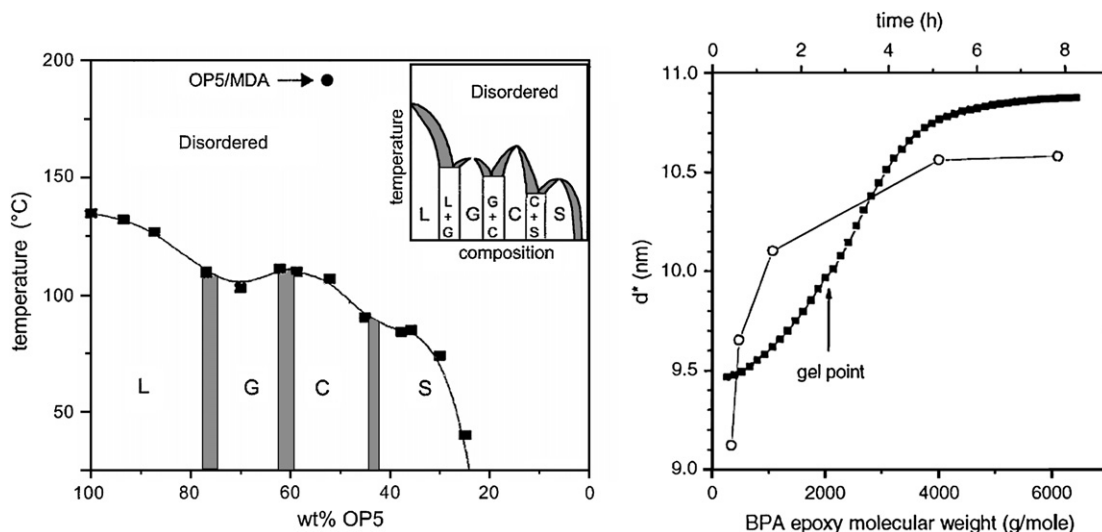
Fig. 2. (Left) Phase diagram for a PEO–PEP diblock in epoxy resin, the inset is a suggestion of what the complete diagram may look like (L = lamellar, G = gyroid, C = hexagonally packed cylinders, S = spheres). (Right) Variation of d-spacing in the 52 wt% diblock system with increasing epoxy molecular weight (open circles) and with cure (filled squares) [38]. Reproduced by permission of the American Chemical Society.
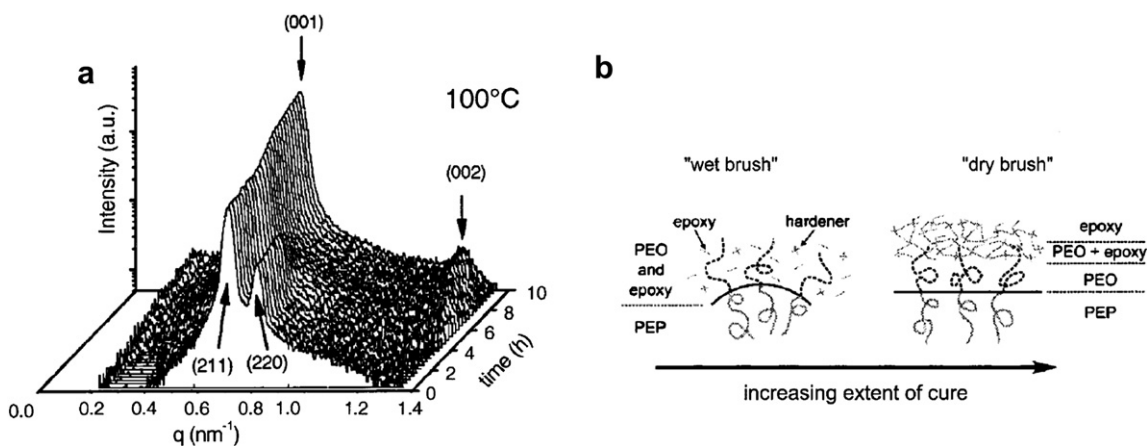

Fig. 3. (a) Time resolved SAXS during cure for a PEO–PEP diblock in epoxy (69 wt%) showing gyroid–lamellar transition. (b) Diagrammatic representation of a possible explanation – expulsion of PEO from epoxy leads to reduced interfacial curvature [38]. Reproduced by permission of the American Chemical Society.

autocatalytic process. It was suggested that this interference is due to preferential hydrogen bonding between the hydroxyl groups on the resin and the PEO oxygens, thus inhibiting autocatalysis. Reaction rate was found to decrease both with increasing block copolymer content in the resin and with increasing PEO content in the block copolymer.

Regarding the interfacial region Sun et al. [46] investigated the composition of the interfacial region using magic-angle spinning nuclear magnetic resonance spectroscopy (MAS-NMR). They were able to confirm the presence of an interphase layer in cured 40 wt% PEO–PPO–PEO/epoxy + MDA blends. They suggest that the interphase is composed of partially dewetted PEO and partially cured epoxy resin. Using spin-diffusion experiments, they were able to estimate the dimensions of the interphase. A diagram of the proposed structure, with dimensions, is shown in Fig. 5. This is consistent with the model proposed by Lipic et al. [38] and shown in Fig. 3(b). On the basis of Lipic et al. initial work the interphase thickness appears to be independent of miscible block length. The core dimension is dependent on the immiscible block length, as expected. We note that the overall dimension of 2.7 nm given for the EO80 blends is notably smaller than the 10–30 nm structures observed by Guo et al. [41] in the same system. It is possible that the

larger structures are aggregates of smaller spherical or wormlike micelles, measured in the NMR experiment and this is borne out by the AFM images in Fig. 4.

2.1.1.2. Studies with other block copolymers. Kosonen et al. have studied phenolic resin modified with poly(2-vinylpyridine)-*b*-polyisoprene [55,56]. Via TEM imaging, they observed microphase separation with a spherical morphology from 5 wt% to 20 wt%, cylinders at 30 wt% and lamellae at 40 wt% (M_n(P2VP) = 21 000 g mol^{-1}; M_n(PI) = 71 000 g mol^{-1}). Reducing the size of the miscible P2VP block to match the molecular weight of the resin monomers lead to significant swelling of the P2VP block. Infrared spectroscopy indicated hydrogen bonding between P2VP and the resin which remained present after cure.

Guo et al. [49] modified a poly(propylene glycol) type epoxy resin with polystyrene-*b*-polybutadiene copolymer. Since neither the polystyrene block nor the polybutadiene block were miscible with the cured epoxy macrophase separation was observed in all blends. Isolated domains of copolymer were observed at 5–10 wt%, bicontinuous interpenetrating phases were formed for 20–60 wt% and at 70 wt% and above, domains of resin in a block copolymer matrix were observed.
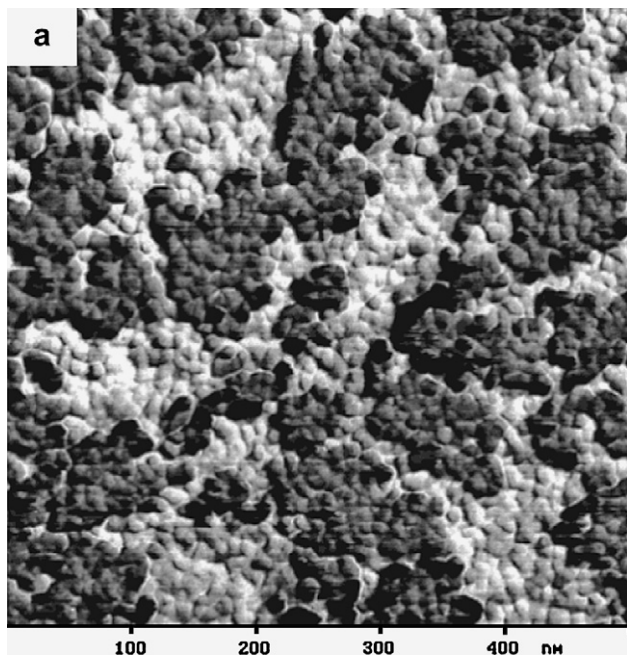
Fig. 4. AFM phase image of 20 wt% PEO–PPO–PEO (80% PEO) cured in epoxy resin. The lighter areas are harder (epoxy-rich) and the dark areas (copolymer-rich) were softer [41]. Reproduced by permission of the American Chemical Society.

ABC triblock copolymer blends have been studied by Ritzenthaler et al. [53,54]. A polystyrene-b-polybutadiene-b-poly(methyl methacrylate) SBM triblock (22–9–69% by weight) was studied in MCDEA cured BADGE. An interesting 'raspberry-like' spheres-on-spheres morphology was observed (Fig. 6a). When changing the hardener to DDS, macrophase separation occurred, with the sphere-on-sphere inclusions remaining stable in the block copolymer phase whilst the epoxy phase separated (Fig. 6c). A second block copolymer with increased polybutadiene content (12 wt% PS, 18 wt% PB, 70 wt% PMMA) was shown to form 'onion-like' multilayered ovular inclusions (Fig. 6d).

An investigation into crystallisation in nanoscale domains was performed by Guo et al. [57] using a diblock copolymer with a crystallisable immiscible block. A PEO–PE diblock with 50 wt% PEO content and M_n of 1400 g mol^{-1} was used to modify a BADGE + MDA resin. Macrophase separation did not occur in any of the cured blends. 5–30 wt% blends of diblock with epoxy show micellar inclusions with increasing packing density. At 40–50 wt% the micelles aggregate and merge to form bicontinuous structures. Above 50 wt% the samples are volume filled with PE and PEO

crystallites. Melting and crystallisation were monitored by DSC and three distinct curing regimes were observed, coinciding with the three morphological regions.

2.1.1.3. Reaction induced microphase separation. In the systems described previously, nanoscale structures are formed in solution and 'fixed' during cure. Although some systems demonstrate a change of morphology during cure all of the systems present some pre-cure structure. As mentioned above, homopolymers can undergo reaction induced macrophase separation. Thus, it is not unreasonable to start with a diblock where both blocks are miscible with the epoxy but where one block separates by a reaction induced mechanism during cure. Meng et al. have demonstrated this behaviour by using a poly(ε-caprolactone)-b-polybutadiene-b-poly(ε-caprolactone) triblock in two recent papers [58,59].

Fig. 7 shows the results from an initial experiment with a poly-(ε-caprolactone)-b-polybutadiene-b-poly(ε-caprolactone) triblock. The scattering data indicate clearly that a micelle structure is formed in the mixture prior to cure since the precursors of epoxy behave as the selective solvent for the triblock copolymer at room temperature. The scattering peak disappeared when the system was heated to 80 °C or higher implying that the micelle structure was destroyed at elevated temperature. With the curing progressing at 150 °C, the microphase-separated structure reappeared as shown by the presence of the well-defined scattering peak (see curve C). It is worth noticing that the long period of the cured sample (ca. 31.4 nm) is significantly higher than that of the blend prior to cure (ca. 11.6 nm). These results indicated that at the curing temperature the curing reaction was indeed started from the homogeneous solutions comprised of the epoxy precursors and triblock copolymer [59].

Similar data were obtained for a PEO–PS diblock. Structure is present in solution in BADGE but disappears on addition of hardener, after cure multiple order scattering peaks are observed and nanostructure is visible by AFM. In this work, higher concentrations of copolymer were also examined although pre-cure data are only provided for the 10 wt% blend [58].

2.2. Reactive block copolymers

In the work examined so far the formation of microphase-separated nanostructures as opposed to macrophase separation relies on balancing thermodynamics and kinetics. Whilst this allows for behaviour such as the reaction induced microphase separation described above, it also limits the range of cross-linking agents and curing conditions that can be used. By designing the block copolymer so that the epoxy-miscible block is reactive towards the epoxy resin or cross-linker, the structure can be fixed before macrophase separation occurs. Chemically bonding the

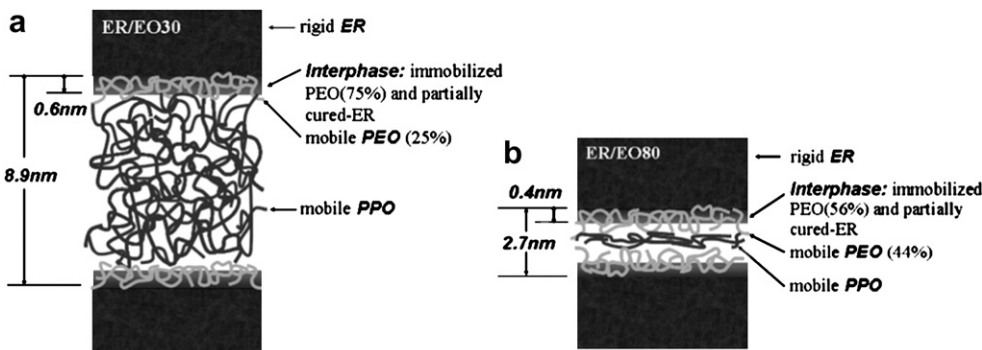**Fig. 5.** Phase dimensions calculated by spin-diffusion MAS-NMR. EO30 is PEO$_{20}$PPO$_{70}$PEO$_{20}$; EO80 is PEO$_{76}$PPO$_{29}$PEO$_{76}$ (where the subscript indicates the number of repeat units) [46]. Reproduced by permission of the American Chemical Society.
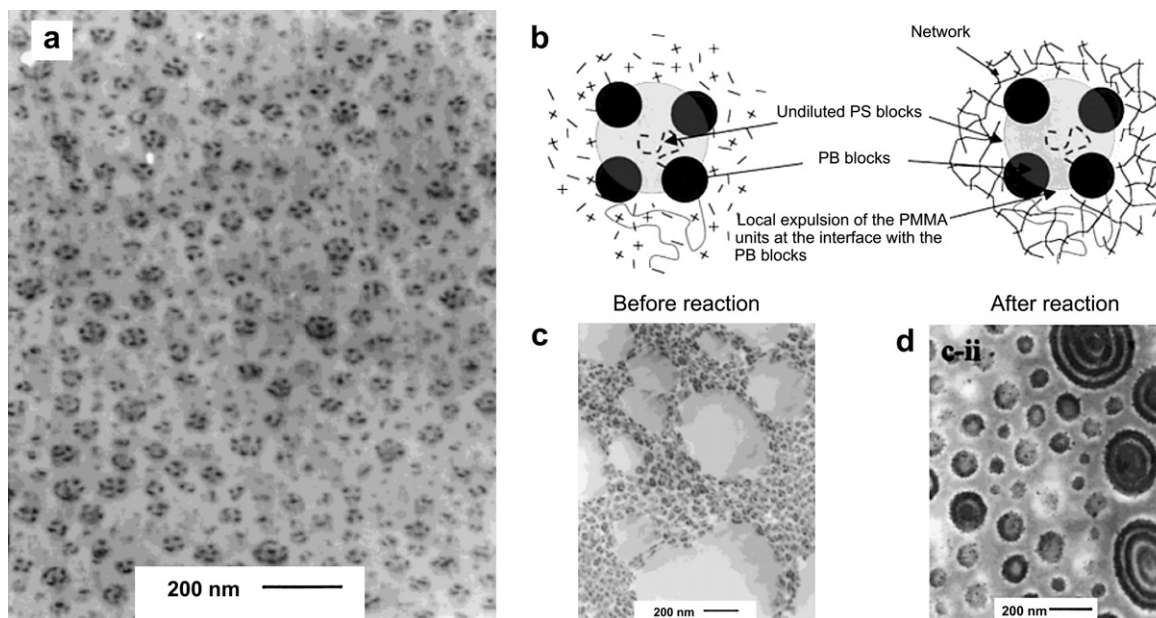
Fig. 6. (a) TEM showing 'raspberry-like' morphology in 50 wt% of SBM copolymer cured with MCDEA; (b) a schematic representation of the structure. (c) The same system cured with DDS showing macrophase separation whilst maintaining nanoscale morphology. (d) TEM of SBM copolymer with higher B content showing 'onion-like' morphology. TEM samples are stained with OSO₄. PB is darkest, PS is weakly stained, PMMA and the resin are unstained [53,54]. Reproduced with permission from the American Chemical Society.
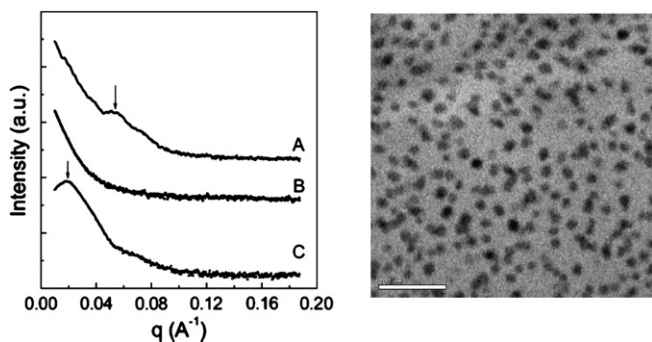

Fig. 7. Reaction induced microphase separation in 10 wt% PCL–PB–PCL in BADG-E + MOCA. [Left] (A) Uncured blend at 25 °C; (B) uncured blend at 150 °C (start of cure); (C) cured thermoset. (Right) TEM image of the cured thermoset; dark spots are OsO₄ stained PB domains, the scale bar is 100 nm [59]. Reproduced by permission of the American Chemical Society.

block copolymer to the resin could also lead to a greater degree of toughening of the epoxy system.

Studies of reactive block copolymers in epoxy resins were undertaken by Grubbs et al. [48]. The polyisoprene block of a poly-isoprene-b-polybutadiene was selectively epoxidised [65] to yield the block structure shown in Table 1 as ePI. The phase behaviour of this block copolymer (75 wt% ePI) in a BADGE + MDA epoxy system was examined and determined to be similar to that for the previously studied PEO–PEP. Micelles were observed at low concentration, followed by packed spheres, hexagonal phase and lamellar structures. A high degree of epoxidation (≥87%) was necessary to ensure miscibility of the ePI block with the resin. Copolymers with low degrees of epoxidation (<75%) were immiscible with epoxy even prior to cure. At 75% epoxidation the block copolymer is initially miscible but undergoes reaction induced macrophase separation during cure. The curing reaction was analyzed by DSC and it was determined that the ePI epoxides react significantly slower than those in the resin. In this way the polyisoprene block selectively epoxidised in ePI remains free to macrophase separate

until it is inhibited by the rigidity of the resin, just as for non-reactive block copolymers. The low reactivity of ePI is due to the highly substituted nature of the ePI epoxide, located as it is on the chain backbone. To overcome this problem, poly(methyl acrylate-co-glycidyl acrylate)-b-polyisoprene copolymers were synthesised. Here, the epoxy group is pendant from the chain. Again, micelles were observed at low concentration and packed more closely as the concentration was increased. DSC analysis revealed a single reaction exotherm, suggesting that the copolymer epoxide has similar reactivity to the BADGE epoxide.

Serrano et al. have recently analyzed linear polystyrene-b-polybutadiene with epoxidation of butadiene block ePB (below and above 40%) in a BADGE + MCDA matrix [66]. These systems formed microphase-separated structures in the uncured state. It was reported that the reactive ePB remains mostly miscible (below and above 40% epoxidation) with the thermosetting resin during reaction. Thus the nanostructure occurs via an epoxy-miscible block (instead of an epoxy-reactive block). The ePB reactivity was slower than that of the epoxy groups in BADGE. For a 30 wt% block copolymer concentration the epoxy system structure consisted of wormlike and hexagonally packed cylindrical micelles for degree of epoxidation below and above 40%, respectively. An increase in toughness was reported in the case of cylinder morphology.

Rebizant et al. [62] have investigated versions of the SMB triblocks that were studied by Ritzenthaler as described above [53,54]. Initially [62] they synthesised an SBMG tetrablock (polystyrene-b-polybutadiene-b-poly(methyl methacrylate)-b-poly-(glycidyl methacrylate)). It was determined that the raspberry morphology could be formed and fixed into cured epoxy in the BADGE + DDS system where previously macrophase separation had been observed. It was also determined that as long as the G block is sufficiently short these systems appear to phase separate as SB(MG) triblocks. In later work [63], they examined polystyrene-b-polybutadiene-b-poly[(methyl methacrylate)-stat-(tert-butyl methacrylate)] (SBMT) and the product of hydrolysis of the tert-butyl methacrylate block to give a poly[(methyl methacrylate)-stat-(methacrylic acid)] block (SBMA triblock). Carboxylic acids are
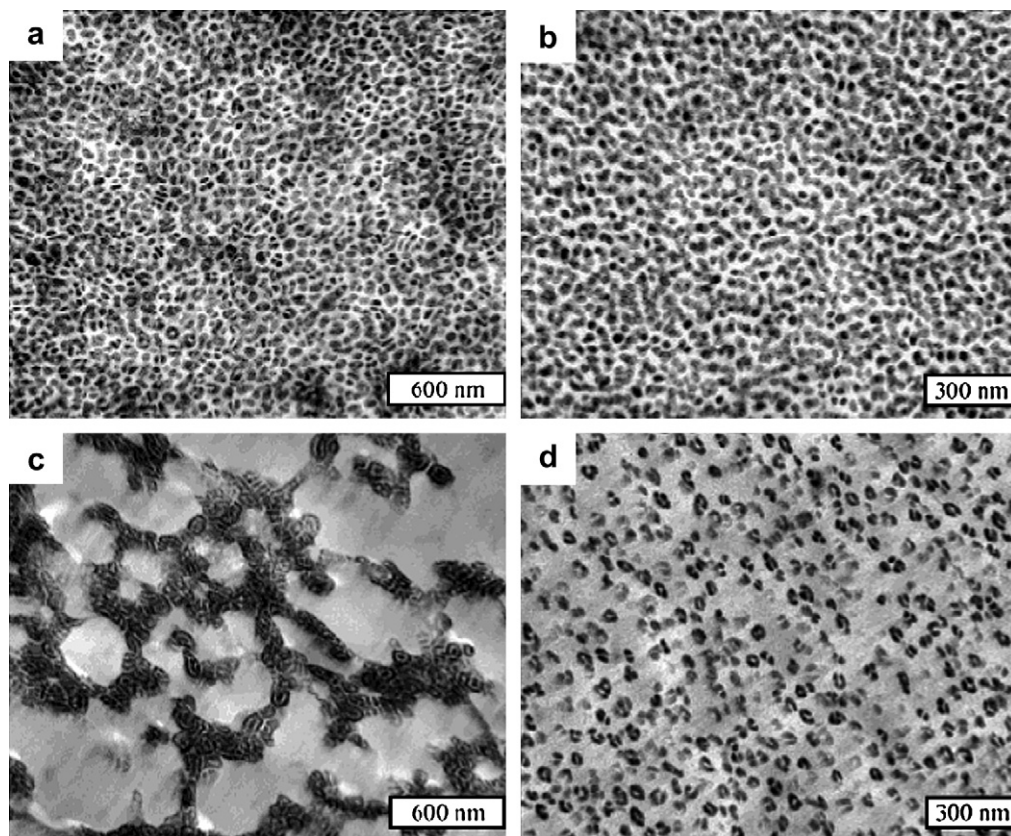
Fig. 8. TEM images of SBMT (left) and equivalent SBMA (right) triblock copolymers at 30 wt% in BADGE + DDS before (top) and after (bottom) cure at 135 °C showing the effect of reactive groups in the epoxy-miscible block [63]. Reproduced by permission of the American Chemical Society.

reactive with epoxide groups as well as with some cross-linking agents. The SBMT triblocks were found to flocculate into visible structures on curing with most hardeners (except MCDEA) whereas the SBMA triblocks maintained their micellar structure (Fig. 8). The method of hydrolyzing a polyester to give a reactive acid group may offer an advantage over the addition of a glycidyl methacrylate block. The latter can only be achieved using a limited range of polymerization conditions owing to the reactivity of the monomer. By contrast, polyesters can be synthesised using a range of techniques and made reactive by hydrolysis after polymerization, providing an attractive route to commercial materials.

3. Toughening

Epoxy resins cured using aromatic cross-linking agents usually have high glass transition temperatures. Whilst this is a desirable property for many applications, it also means that unmodified cured resins can be extremely brittle. Traditionally, toughening (i.e. resistance to the propagation of a sharp crack) is achieved using rubbery modifiers which are either thoroughly immiscible with the epoxy or undergo reaction induced macrophase separation [67–71]. In recent years, theoretical understanding regarding toughening mechanisms has been advanced. Some reviews [72–74] gave detailed descriptions of the existing toughening mechanisms used to explain the improved toughness for modified epoxy resins. We briefly discuss below the main toughening mechanisms.

Shear yielding [24,71,75] is a major mechanism proposed for second phase modified polymers, especially when the fillers are of a rubbery nature. It involves matrix deformation and cavitations of the particles in response to the stresses near the crack tip. In

addition, there is shear yielding between the holes formed by the cavitated rubber particles. Plastic deformation blunts the crack tip, consequently the local stress concentration is reduced allowing the material to support higher loads before failure occurs. For this reason the major energy absorption mechanism is suggested to be the plastic deformation of the matrix.

In the particle bridging mechanism [76] rigid or flexible particles play two roles: (a) they act as bridging particles granting compressive grip in the crack path and (b) the ductile particles deform plastically in the material surrounding the crack tip providing additional crack shielding. The particle bridging is held to be responsible for most of the improvements in toughness.

A crack-pinning mechanism [77] proposes that as a crack propagates through the resin, the crack front bows out between the second phase dispersion and remains pinned at the positions where it has encountered the particles.

The microcracking mechanism [78,79] supposes that incorporating rubber into polymers creates microcracks caused by the presence of the fillers. Such microcracks provide improved toughness and originate tensile yielding, thus a large tensile deformation. Voids result when the microcracks open, and permit large strains. Debonding effectively lowers the modulus in the frontal zone around the crack tip therefore reducing the stress intensity there.

All the toughening mechanisms proposed above have their attractive features but none are compelling in their wide applicability.

It is worth noting that several studies report fracture toughness in terms of the strain energy release rate, G_c. For a linear elastic fracture mechanism a simple relationship exists for G_c and critical stress intensity factor K_{1c} for plane-strain conditions [1]

$$G_c = \frac{K_{1c}^2}{E}\left(1 - v^2\right) \tag{1}$$

where E is the Young's modulus and v the Poisson's ratio of the sample. The Poisson's ratio is normally taken to be constant for all samples in a given set. Since variation in E is generally undesirable it is best recorded separately from fracture toughness. Discussion here is limited to changes in critical stress intensity factor K_{1c} only.

It is often found in practice that the measured values of toughness are dependent on specimen thickness, over a range of thicknesses until a critical dimension is reached. Once the thickness exceeds the critical dimension, the value of stress intensity factor K_1 becomes relatively constant $K_1 \to K_{1c}$ being a true material property. The thickness effect arises because the state of stress near the crack tip varies from plane-stress in the surface region of thin plates to plane-strain in relatively thick plates away from the free surfaces [24]. A characteristic form of the relationship between stress intensity factor K_1 and specimen thickness B is shown in Fig. 9 where it can be seen that K_1 values at plane-stress condition are higher than those under plane-strain conditions.

It should be noted that K_{1c} is often referred to as the plane-strain fracture toughness, e.g. ASTM-E 399 [80]. In plane-strain conditions, materials behave essentially elastically until the fracture stress is reached and then rapid fracture occurs. This mode of fracture is named brittle fracture because little or no plastic deformation is observed.

A critical account of the data in the literature is needed as K_{1c} values are rarely recorded in conditions that fulfil the plane-strain criteria. Thus the values are exaggerated i.e. for a toughened sample a different geometry is required. According to Williams [81] the plane-stress criterion for specimens of thickness B is

$$B > 2.5\left(\frac{K_{1c}}{\sigma_y}\right)^2 \tag{2}$$

where σ_y is the yield stress.

Ryan et al. reported in 1991 [82] the difference observed in the fracture surface of poly(urethane–urea) specimens under plane-stress and plane-strain conditions. The tested specimens had beam geometry of the same thickness but different composition. Fig. 10(a) and (b) shows brittle featureless fracture surfaces presenting little damage. These materials were tested under conditions approximating to plane-strain (σ_y were 17 and 25 MPa,

Fig. 10. Comparative scanning electron micrographs of the fracture surfaces of poly-(urethane–urea) specimens with different hard segment composition prepared by reaction injection moulding: (a) 61% hard segment content; (b) 51% hard segment content; (c) 35% hard segment content. The brittle fracture surfaces in (a) and (b) correspond to plane-strain condition while the ductile fracture surface in (c) accounts for plane-stress condition [82]. Reproduced by permission of Elsevier Ltd.

respectively). In contrast Fig. 10(c) shows ductile fracture surfaces with yielding and tearing ($\sigma_y < 15$ MPa), in this case plane-stress condition prevailed. Single notch fracture tests were performed for a full range of poly(urethane–urea) with various hard segment content φ_{HS} (Fig. 11). The specimens under plane-stress condition $\varphi_{HS} < 0.5$ that showed ductile fracture surfaces (Fig. 10(c)) yielded $G_{1c} > 6$ KJ m^{-2}. Conversely for $\varphi_{HS} > 0.5$, $G_{1c} < 3$ KJ m^{-2} consistent with the brittle fracture surface in Fig. 10(a) and (b). At $\varphi_{HS} \sim 0.5$ there seemed to be a transition in fracture properties that is an artefact due to specimen geometry. In much of the published work, especially in the field of polymer fracture, it is not always possible to determine whether the quoted values of K_{1c} are truly plane-strain values.

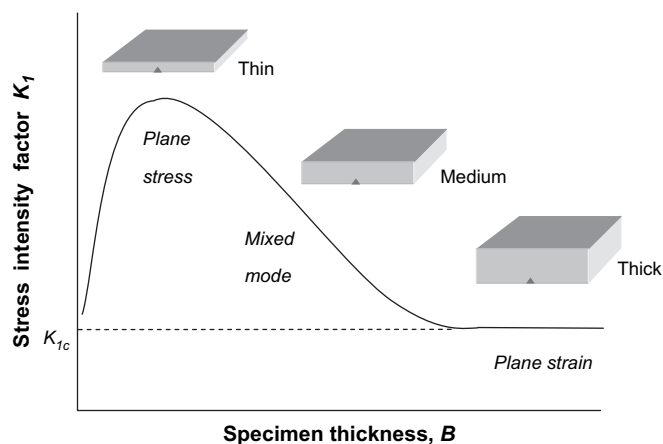**Fig. 9.** Schematic diagram showing the variation of the measured stress intensity factor K_1 as a function of specimen thickness B. The material is under plane-stress, mixed mode and plane-strain condition when the specimen thickness is thin, medium and thick, respectively. In plane-strain condition and for a relatively thick specimen, the stress intensity factor K_1 becomes constant $K_1 \to K_{1c}$. Redrawn from Ref. [24].
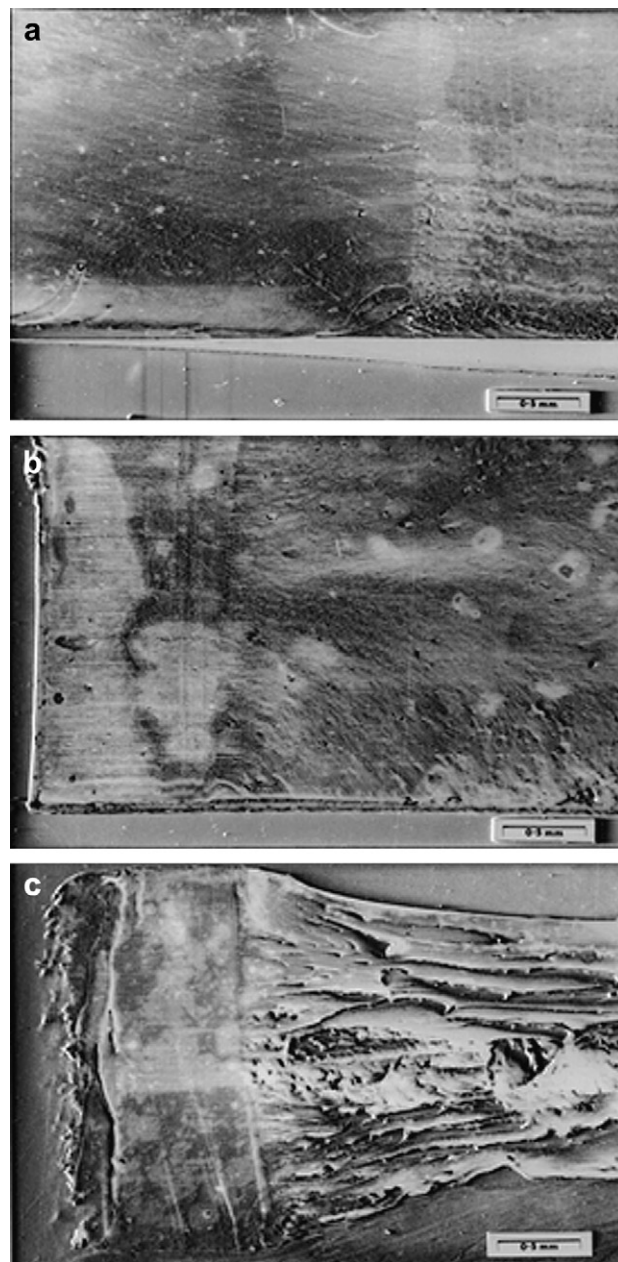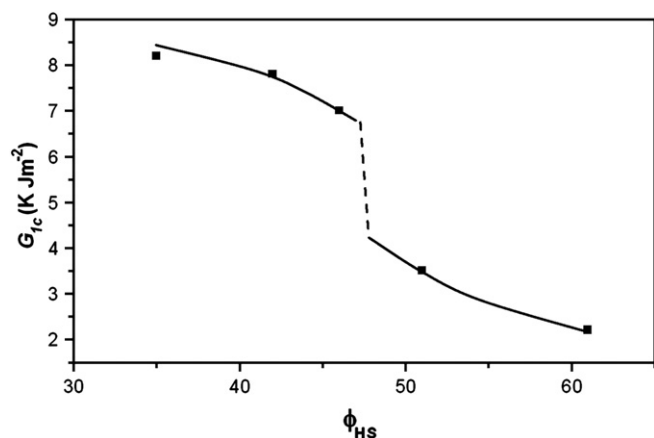
Fig. 11. Plot of G_{1c} versus hard segment composition φ_{HS} for reaction injection moulding poly(urethane–urea). At $\varphi_{HS} \sim 0.5$ there seems to be a transition in fracture properties; for $\varphi_{HS} < 0.5$ G_{1c} values are greater than those for $\varphi_{HS} > 0.5$. Fig. 10(a)–(c) fracture surfaces yield the points shown in the plot for $\varphi_{HS} > 0.5$ (plane-strain) and $\varphi_{HS} < 0.5$ (plane-stress) [82]. Reproduced by permission of Elsevier Ltd.

In systems modified with traditional additives the level of toughening achieved and the effect on the mechanical properties of the cured resin are dependent on the curing conditions. The morphology adopted by block copolymer modified systems should largely be determined by the composition of the modifier. Thus it has been suggested that these systems may give reproducible levels of toughening over a much wider range of curing conditions.

Dean et al. [39] studied the effect of PEO–PEP block copolymers at low concentration on a BADGE + MDA system. Spherical micelles were found to improve fracture toughness K_{1c} by 25–35%. No statistically significant link was found between micelle radius and improvement in K_{1c}. A vesicular morphology was found to increase K_{1c} by 45% even at half the block copolymer concentration of the micelle forming systems. It was suggested that the resin inside the vesicle acts as a separated microparticle in a similar way to phase-separated modifiers. The bulk of the modifying particle essentially consists of epoxy with only the vesicle walls containing block copolymer. Thus, lower modifier concentrations are required to achieve a similar degree of toughening as that reached by micelle forming polymers i.e. the fracture toughness is altered by the effective volume of the toughening particles.

In a further paper [52] non-reactive PEO–PB copolymers are compared to ePI–PB and polymers with a reactive P(MA-*co*-GMA) epoxy-miscible block. ePI–PB and reactive epoxy-miscible P(MA-*co*-GMA) block form nanoscale structures which are chemically bonded to the resin after and before gelation of the epoxy resin, respectively. Again, vesicles were found to be best at improving fracture mechanics (quoted as improvement in G_c only). Non-reactive vesicles provided poorer toughness than the vesicles in which the ePI block was 'stitched' to the resin after gelation. Consecutively, superior toughness was achieved using P(MA-*co*-GMA) based diblocks which were 'stitched' to the resin before gelation had occurred.

Seemingly conflicting results were obtained in a study using PEO–PEP and reactive block copolymers in partially brominated BADGE resins cured with phenol novolac [40]. Spherical micelles were found to give significantly greater improvements in toughness than vesicles. Even greater enhancement was found when wormlike micelles were formed ($\sim 4\times$ improvement in K_{1c}; $\sim 3\times$ with spherical micelles). The relative improvement in toughness was found to increase as brominated epoxy content increased. Increased bromination leads to a more brittle resin in the absence of toughening agent. Enhanced brittleness means thinner samples

are needed for plane-strain condition. Wu et al. observed similar behaviour when they studied PEO–PBO diblock copolymers in non-brominated BADGE + phenol novolac [37]. Again, wormlike micelles were found to prove the greatest improvement in K_{1c} ($\sim 4\times$) followed by spherical micelles ($\sim 2.5\times$) and vesicles ($\sim 1.8\times$). It is suggested that the toughening observed with micelles may be due to cavitation processes. With wormlike micelles, scanning electron microscopy (SEM) indicates that worms bridging the crack are 'pulled-out'. There is also evidence for nanometre scale crack deflection leading to the detachment of thin flakes of epoxy from the fracture surface.

Very recently, Thio et al. have reported the behaviour of poly-(ethylene oxide)-*b*-poly(hexylene oxide) (PEO–PHO) diblocks in phenol novolac cured BADGE [83]. The highly non-polar PHO block is immiscible with BADGE even at low molecular weights. Worm-like micelles were generated by mixing a vesicle forming diblock (9 wt% PEO) and a spherical micelle forming diblock (44 wt% PEO). Here the wormlike morphology, shown in Fig. 12, was again found to give the best improvement in K_{1c} ($\sim 6\times$), but vesicles were found to give greater improvements than spherical micelles ($\sim 3.5\times$ and $\sim 1.75\times$, respectively). These improvements in properties have to be considered in the context of whether the measurement fulfilled the condition of plane-strain. In this particular work values of K_{1c} and E were provided hence the minimum thickness B could be calculated with the aim of testing whether the plane-strain criteria were fulfilled. σ_y can be determined from E as for most solids $\sigma_y^{theoretical} \approx E/10$. However, the measured values of yield stress σ_y are invariably much less than $E/10$ for most materials due to the presence of flaws [84–87]. They are typically in the order of $E/50$ to $E/100$ for isotropic polymers. For typical thermosetting polymer (epoxy resin) $E = 3500$ MPa, $\sigma_y^{theoretical} = 350(MPa)$ and the calculated $\sigma_y = 70$ MPa, which is $E/50$ r. Therefore taking $\sigma_y \sim E/50$ and applying Eq. (2) the minimum thickness necessary for plane-strain would be $B > 5.7$ mm for wormlike micelles, $B > 0.537$ mm for micelles and $B > 4.23$ mm for vesicle conformation. Since the tested specimens were bars of 40 mm gauge length and 3.2 mm $\times$ 3.2 mm cross-section r the measurements for wormlike and vesicle conformation were performed in conditions of plane-stress instead of plane-strain. This means that the K_{1c} values
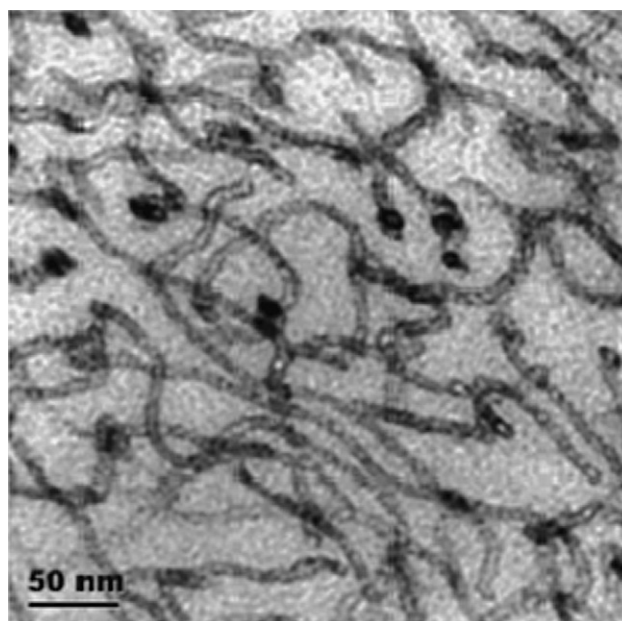

Fig. 12. TEM image showing wormlike micelles of PEO–PHO in a BADGE + PN system. Stained with RuO$_4$ [83]. Reproduced by permission of the American Chemical Society.

reported for wormlike micelles and vesicles are exaggerated with respect to those obtained under plane-strain conditions for the micellar system.

Ritzenthaler [54] and Rebizant [63] have reported maximum K_{1c} improvements of around 2× by particles forming the 'spheres-on-spheres' morphology described above.

Whilst it is suggestive to report toughness values for samples with the same thickness it should be noted that these are not always the plane strain fracture toughness. It could well be that one toughening morphology appears to be much better than another. This is because of the combination of the sample geometry and the material's properties shift the measurement regime from plane strain to plane stress. For a given sample geometry one needs to know both the measured value of K_{1c} and the yield stress to be sure that plane-strain conditions have been satisfied.

From the point of view of interactions between matrix and filler, soft and rigid nanofillers behave differently. Soft particles must be adequately bonded to the matrix in order to be effective energy absorbers behind a crack front. Alternatively, when there is a weaker interface an expanding crack translates into extraction of nanoparticles from the surrounding matrix. Such pull-out or extraction from the matrix is associated with friction and energy dissipation which translates into substantial toughness [88]. In polymers containing rigid particles it is not always necessary to have a good degree of particle/matrix adhesion for the material to have optimum mechanical properties. In this case the degree of adhesion is controlled by the particle modified surface and their interaction with the matrix.

An important challenge in nanocomposite production is the understanding of materials that allow the transfer of the excellent mechanical properties (i.e. tensile strength and Young's modulus E) of the nanofillers to the macroscale properties of the bulk matrix. Following this argument, the downside of PNC is that their mechanical properties drop below the calculated theoretical and experimentally determined values of the individual nano-inclusions, except at low volume fractions of the second phase [22,89–95]. In general, it can be concluded that four important structural parameters must be maximized in order to obtain optimal PNC. These parameters are: (a) particle–aspect ratio, (b) particle packing (or alignment), (c) particle dispersion and (d) polymer-to-particle interfacial stress transfer.

As we report here, the morphology (i.e. vesicles, micelles or wormlike micelles) adopted by block copolymers in the modified resins has a major influence on K_{1c}. Although these results are promising they are still far from replicating the high toughness of biological composites found in nature such as wood, bone or nacre. Biological nanocomposites owe their toughness mostly to the incorporation of structural artefacts. These can be the intricate hierarchical architecture that incrementally develops at higher scales (in nacre and bone) and the soft interfaces at various scales (in bone) [96–98].

A traditional approach adopted by nanotechnology is the attempt to reproduce synthetically in the laboratory the complex biological systems existing in nature. In this fashion an impressive breakthrough has been reported very recently by Posiadlo et al. [99]. This work demonstrates the exceptional mechanical properties of a multilayer montmorillonite (MTM) clay nanoplatelets/polymer nanocomposites prepared with a layer-by-layer assembly process. The polymer matrix was a poly(vinyl alcohol) (PVA). The layer-by-layer assembly process yielded a resulting composite strongly reminiscent of the biological nanocomposites described previously. However, the packing perfection in biological composites was still higher. The MTM/PVA nanocomposites displayed ∼four times higher strength and nearly one order of magnitude higher modulus when compared with pure PVA polymer. It remains to be seen if this layer-by-layer preparation technique can be successfully applied to thermoset resins such as epoxy. It is clear that a deeper understanding of the physical phenomena occurring at the filler/matrix interface is crucial for tailoring PNC mechanical properties.

4. Glass transition

The glass transition temperature (T_g) of a non-crystalline (amorphous) material can be defined as the critical temperature above which the material changes its behaviour from being 'glassy' to being 'rubbery'. When an amorphous material is cooled down the segmental mobility decreases until T_g is reached, at that point the system drops out of thermodynamic equilibrium [100]. The resulting material, a glass, relaxes towards thermodynamic equilibrium via a structural relaxation process [101–103] also called physical aging [104,105]. The nature of T_g and the structural relaxation process associated to it are currently considered as major challenges in condensed-matter physics [101,106,107].

As discussed in Section 1, epoxy resins find applications in areas such as coatings, adhesives or matrix materials for composites. The main requirement for these applications is that the material should be a rigid solid at use temperature T_{use}. The use temperature must be below the glass transition temperature $T_{use} < T_g$. Thus, most of the work performed to date involving investigations of nano-structure formation in epoxy resins has been driven by the desire to modify the properties of the bulk material in a commercially useful manner. This includes increasing the glass transition temperature and improving the material fracture toughness, simultaneously if possible.

The morphology adopted by block copolymer modified epoxy systems has an effect not only on the resin mechanical properties but also on its glass transition temperature.

PEO–PEP and reactive block copolymers in partially brominated BADGE resins cured with phenol novolac [40] showed that K_{1c} enhancement was found when wormlike and spherical micelles were formed (∼4× improvement in K_{1c} for wormlike morphology; ∼3× with spherical micelles). Moreover the glass transition temperature increased in the systems containing spherical and wormlike micelles. This is contrary to what one would intuitively expect and has not been fully explained. Nevertheless, it was suggested that the presence of PEO may enhance the cross-linking in some way, hence reducing polymer segment mobility and increasing T_g.

Wu et al. observed similar behaviour when they studied PEO–PBO diblock copolymers in non-brominated BADGE + phenol novolac [37]. The glass transition was again seen to rise after modification, with the greatest increase for the wormlike morphology. They speculated that the increase in T_g may be due to localised concentration fluctuations of epoxy and hardener when blended with diblock, leading to a modified network structure. Thio et al. also reported the behaviour of poly(ethylene oxide)-*b*-poly-(hexylene oxide) (PEO–PHO) diblocks in phenol novolac cured BADGE [83]. Again there appears to be some correlation between T_g and the improvement in K_{1c}.

Despite the fact that T_g is usually quoted and accepted as single numerical value, different methods of measurement and sample preparation will provide varying data for the same material. Differential scanning calorimetry (DSC) is the simplest method. Such a technique consists of heating the sample in a closely calibrated furnace where the temperature of the sample is compared to the temperature of a blank reference cell. Thermodynamic transitions such as melting points and reaction exotherms can be monitored. The change in heat capacity associated with T_g is seen as a shift in the baseline for cured resins. A drawback is that, high filler loadings, high cross-link densities, and other thermo-molecular
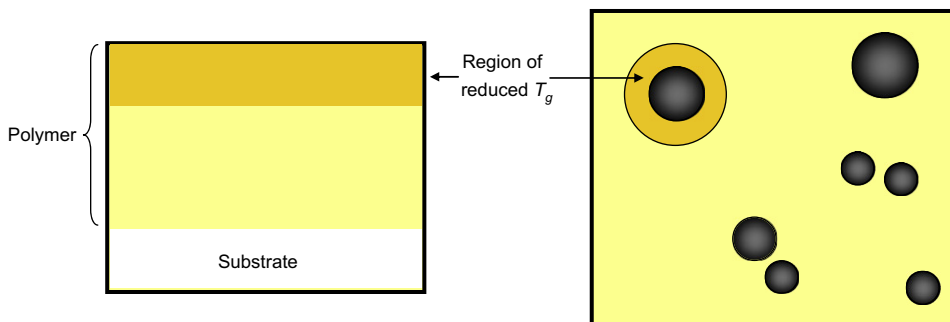
Fig. 13. Schematic cross-section of a polymer thin film on a substrate (left) and a polymer nanocomposite (right) having equivalent surface-to-volume ratios. Shaded regions represent material displaying a glass transition temperature below the bulk value due to enhanced mobility [8]. The work of Bansal et al. [6] reveals a similar suppression of T_g in the confined geometries of polymer–particle nanocomposites and thin films. Adapted by permission of Macmillan Publishers Ltd.

processes can mask the shift due to the T_g and make the transition difficult or impossible to identify. Dynamic mechanical analysis (DMA) consists of oscillation force applied to a rectangular bar of the composite. The stress that is transferred through the specimen is measured as a function of temperature. From the deformation of the sample under the load, the stiffness can be determined, and the sample modulus can be calculated. In addition, it is possible to determine the damping properties (tan δ) of the material. Different routines for defining T_g can be used, such as [1,108,109] the following.

1. The temperature of the maximum in the mechanical tan δ peak
2. The point of inflexion of log E' versus T curve or the 'mid'point of the transition, where E' is the Young's modulus real component (storage modulus)
3. An intercept method.

There can be large differences between the T_g estimates depending on the method used. DMA can also resolve sub-T_g transitions, like beta, gamma, and delta transitions whereas in many materials the DSC technique is not sensitive enough to detect these phenomena.

It is important to mention that within the same sample, the glass transition occurs over a range of temperatures and not as a single value. Aspects such as intrachain stiffness, polar forces, and comonomer compatibility can affect the size of the glass transition region [110]. Hence, DSC and DMTA can be described as elementary techniques as they only offer an average of the different T_g values present over the specimen.

Using computer simulations Starr et al. [111] reported that the thermomechanical behaviour of polymers with regularly spaced nanoparticles should be similar to thin polymer films. Embedding non-interacting nanoparticles in a polymer matrix causes segments in the particles' vicinity to relax faster. This is due to the enhanced chain mobility in the vicinity of the inclusions' surface and is responsible for a local T_g reduction. The local T_g reduction is found to be valid regardless of whether the polymer wets the filler or not [111]. Such result is clearly reminiscent of the findings of Ellison et al. [7,112,113].

In the case of substrate supported thin polymer films, fluorescence experiments performed by Ellison and Tokelson [113] showed a T_g suppression in the free surface with improved segment mobility. It was also reported that layers deeper within the film are affected by the presence of the free surface. Conversely, close to the substrate, T_g decreased with decreasing film thickness. Their findings suggest that the two interfaces of the film are in dynamic 'communication' when sufficiently close together instead of following a two layer-model behaviour.

Inspired by the simulations of Starr et al. [111], Bansal et al. [6] determined the T_g values of polystyrene/silica nanocomposites at several nanoparticle contents. Subsequently, these values were compared to T_g values reported in the literature for polystyrene thin films. It was shown that the way silica nanoparticles suppress T_g quantitatively mimics T_g shifts observed when polystyrene is confined in a thin film geometry, if the interparticle distance is equal to the film thickness. A schematic representation is shown in Fig. 13. A two layer model given by the presence of modified mobility regions in the particle surface vicinity was not sufficient to explain the glass transition process. As for thin films, it was speculated for nanocomposites that the glass transition suppression process required the interaction of the interphase regions surrounding different inclusions.

One of the key features of this interesting study is the heterogeneous nature of the particle distributions, this is variably sized aggregates dispersed amongst single fillers.

These findings open the following questions: what is the role of particle size for a fixed interparticle distance? Is there an actual particle size below which there is no T_g suppression? What is the extent of the filler loading?

It would certainly be a significant achievement if the fluorescence method employed by Ellison et al. [7,112,113] could be applied to cross-linked polymer nanocomposites. In particular, when block copolymers are used as the second phase, the supposedly enhanced mobility region that surrounds them could be monitored by fluorescent dyes. Such fluorescent dyes, covalently attached to the resinophilic and/or resinophobic block parts and randomly dispersed in the matrix should be able to screen areas with diverse degrees of freedom. The average of T_g values in different points of the same specimen should be similar to that value given by the traditional DSC or DMTA.

As toughened thermosets find themselves in ever more stringent applications it is imperative to gain a deeper understanding of the processes occurring at the interfacial regions surrounding nanoinclusions.

5. Conclusions

Block copolymers are used as the second phase in nanocomposites with the purpose of toughening by the nanostructure. The morphology and behaviour of modified resins involving different matrices, curing agents and block copolymers are reported. The block copolymers reviewed can be divided into three categories. The first type are those that self-assemble in the uncured epoxy via a resinophilic part (epoxy-miscible block) and a resinophobic part (epoxy-immiscible block). The nanoscale structures are formed in the pre-cure stage and fixed during cure.

The second class is formed by the diblocks where both blocks are miscible but one of them undergoes reaction induced microphase separation. The case where the epoxy-miscible block is reactive towards the resin or the curing agent conforms to the third type. The toughness attained with the incorporation of soft nano-inclusions depends on the morphology adopted by the block copolymers. It was reported that a vesicular morphology improved fracture toughness significantly more than a micellar morphology for non-reactive polymers. When comparing reactive with non-reactive inclusions, non-reactive vesicles provided poorer tough-ness than vesicles where one of the blocks was chemically bonded to the matrix. In general for both reactive and non-reactive poly-mers the morphology granting the best toughness was wormlike micelles. The rich data in the literature come with a "health warning" as the nature of materials themselves means that it is often difficult to perform full thickness fracture tests. Such tests grant the material property K_{1c} in plane-strain as opposed to some higher value measured in a sample that was able to locally yield.

The glass transition in block copolymer modified resins was seen to rise in the systems containing spherical and wormlike micelles despite the intrinsically plasticizing nature of the resin-ophilic polymer. This contradictory effect has not been fully explained.

It has also been reported that the thermomechanical behaviour of nanoparticle filled polymers should be similar to thin films. What is still needed is a better understanding of the physical mechanisms occurring at the soft nanoinclusion–matrix interface to interpret the data and tailor polymer nanocomposites.

References

[1] Ellis B. Chemistry and technology of epoxy resins. Blackie Academic & Professional; 1993.
[2] May CA. In: May Clayton A, editor. Epoxy resins: chemistry and technology. 2nd ed. New York, NY: Dekker; 1988.
[3] Johnsen BB, Kinloch AJ, Mohammed RD, Taylor AC, Sprenger S. Polymer 2007;48:530–41.
[4] Jordan J, Jacob KI, Tannenbaum R, Sharaf MA, Jasiuk I. Mater Sci Eng A 2005;393:1–11.
[5] Lee SM. Epoxy resins, chemistry and technology. 2nd ed. New York, NY: Dekker; 1988.
[6] Bansal A, Yang H, Li C, Cho K, Benicewicz BC, Kumar SK, et al. Nat Mater 2005;4:693–8.
[7] Ellison CJ, Torkelson JM. Nat Mater 2003;2:695–700.
[8] Mayes AM. Nat Mater 2005;4:651–2.
[9] Vaia RA, Vaia HD. Mater Today November 2004;32:32–7.
[10] Zhang H, Zhang Z, Friedrich K, Eger C. Acta Mater 2006;54:1833–42.
[11] Friedrich K, Fakirov S, Zhang Z. Polymer composites: from nano-to-macro-scale. New York, NY: Springer; 2005.
[12] Abramoff B, Convino J. J Appl Polym Sci 1992;46:1785–91.
[13] Landry CJT, Coltrain BK, Landry MR. Macromolecules 1993;26:3702–12.
[14] Lee J, Yee AF. Polymer 2000;41:8363–73.
[15] Bagheri R, Pearson RA. Polymer 1996;37:4529–38.
[16] Akita H, Hattori T. J Polym Sci B Polym Phys 1999;37:189–97.
[17] Akita H, Kobayashi H. J Polym Sci B Polym Phys 1999;37:209–18.
[18] Akita H, Kobayashi H, Hattori T, Kagawa K. J Polym Sci B Polym Phys 1999;37:199–207.
[19] Chang JH, An YU. J Polym Sci B Polym Phys 2002;40:670–7.
[20] Magaraphan R, Lilayuthalert W, Siriviat A, Schwank JW. Compos Sci Technol 2001;61:1253–64.
[21] Schaefer DW, Justice RS. Macromolecules 2007:40 (web release 1 Nov 07).
[22] Treacy MM, Ebbesen TW, Gibson JM. Nature 1996;381:678–80.
[23] Vaia RA, Giannelis EP. MRS Bull 2001;26:394–401.
[24] Kinloch AJ, Young RJ. Fracture behaviour of polymers. London and New York: Applied Science Publishers Ltd; 1983.
[25] Alexandridis P, Lindman B. Amphiphilic block copolymers: self-assembly and applications. Amsterdam, Oxford: Elsevier; 2000.
[26] Fairclough JPA, Mai S-M, Matsen MW, Bras W, Messe L, Turner SC, et al. J Chem Phys 2001;114(12):5425–31.
[27] Hadjichristidis N, Pispas S, Floudas G. Block copolymers: synthetic strategies, physical properties, and applications. New York, NY: Wiley; 2003.
[28] Hamley IW. The physics of block copolymers. Oxford: Oxford University Press; 1998.
[29] Hamley IW. Developments in block copolymer science and technology. Chichester: John Wiley; 2004.
[30] Hamley IW. Block copolymers in solution: fundamentals and applications. Chichester: John Wiley; 2005.
[31] Mai S-M, Fairclough JPA, Terrill NJ, Turner SC, Hamley IW, Matsen MW, et al. Macromolecules 1998;31(23):8110–6.
[32] Battaglia G, Ryan AJ. Nat Mater 2005;4(11):869–76.
[33] Hillmyer MA, Lipic PM, Hajduk DA, Almdal K, Bates FS. J Am Chem Soc 1997;119(11):2749–50.
[34] Konczol L, Doll W, Buchholz U, Mulhaupt R. J Appl Polym Sci 1994;54(6): 815–26.
[35] Guo Q, Wang K, Chen L, Zheng S, Halley PJ. J Polym Sci Part B Polym Phys 2006;44(6):975–85.
[36] Mijovic J, Shen M, Sy JW, Mondragon I. Macromolecules 2000;33(14): 5235–44.
[37] Wu J, Thio YS, Bates FS. J Polym Sci Part B Polym Phys 2005;43(15): 1950–65.
[38] Lipic PM, Bates FS, Hillmyer MA. J Am Chem Soc 1998;120(35):8963–70.
[39] Dean JM, Lipic PM, Grubbs RB, Cook RF, Bates FS. J Polym Sci Part B Polym Phys 2001;39(23):2996–3010.
[40] Dean JM, Verghese NE, Pham HQ, Bates FS. Macromolecules 2003;36(25): 9267–70.
[41] Guo Q, Thomann R, Gronski W, Thurn-Albrecht T. Macromolecules 2002; 35(8):3133–44.
[42] Larranaga M, Arruti P, Serrano E, Caba K, Remiro PM, Riccardi CC, et al. Colloid Polym Sci 2006;284(12):1419–30.
[43] Larranaga M, Gabilondo N, Kortaberria G, Serrano E, Remiro P, Riccardi CC, et al. Polymer 2005;46(18):7082–93.
[44] Larranaga M, Martin MD, Gabilondo N, Kortaberria G, Corcuera MA, Riccardi CC, et al. Polym Int 2004;53(10):1495–502.
[45] Larranaga M, Martin MD, Gabilondo N, Kortaberria G, Eceiza A, Riccardi CC, et al. Colloid Polym Sci 2006;284(12):1403–10.
[46] Sun P, Dang Q, Li B, Chen T, Wang Y, Lin H, et al. Macromolecules 2005; 38(13):5654–67.
[47] Guo Q, Dean JM, Grubbs RB, Bates FS. J Polym Sci Part B Polym Phys 2003;41(17):1994–2003.
[48] Grubbs RB, Dean JM, Broz ME, Bates FS. Macromolecules 2000;33(26): 9522–34.
[49] Guo Q, Figueiredo P, Thomann R, Gronski W. Polymer 2001;42(26):10101–10.
[50] Serrano E, Martin MD, Tercjak A, Pomposo JA, Mecerreyes D, Mondragon I. Macromol Rapid Commun 2005;26(12):982–5.
[51] Serrano E, Tercjak A, Kortaberria G, Pomposo JA, Mecerreyes D, Zafeiropoulos NE, et al. Macromolecules 2006;39(6):2254–61.
[52] Dean JM, Grubbs RB, Saad W, Cook RF, Bates FS. J Polym Sci Part B Polym Phys 2003;41(20):2444–56.
[53] Ritzenthaler S, Court F, David L, Girard-Reydet E, Leibler L, Pascault JP. Macromolecules 2002;35(16):6245–54.
[54] Ritzenthaler S, Court F, Girard-Reydet E, Leibler L, Pascault JP. Macromole-cules 2003;36(1):118–26.
[55] Kosonen H, Ruokolainen J, Nyholm P, Ikkala O. Macromolecules 2001;34(9): 3046–9.
[56] Kosonen H, Ruokolainen J, Nyholm P, Ikkala O. Polymer 2001;42(23): 9481–6.
[57] Guo Q, Thomann R, Gronski W, Staneva R, Ivanova R, Stuehn B. Macromol-ecules 2003;36(10):3635–45.
[58] Meng F, Zheng S, Li H, Liang Q, Liu T. Macromolecules 2006;39(15): 5072–80.
[59] Meng F, Zheng S, Zhang W, Li H, Liang Q. Macromolecules 2006;39(2): 711–9.
[60] Zucchi IA, Galante MJ, Williams RJJ. Polymer 2005;46(8):2603–9.
[61] Fine T, Lortie F, David L, Pascault J-P. Polymer 2005;46(17):6605–13.
[62] Rebizant V, Abetz V, Tournilhac F, Court F, Leibler L. Macromolecules 2003;36(26):9889–96.
[63] Rebizant V, Venet A-S, Tournilhac F, Girard-Reydet E, Navarro C, Pascault J-P, et al. Macromolecules 2004;37(21):8017–27.
[64] Matsen MW. Macromolecules 1995;28(17):5765–73.
[65] Grubbs RB, Broz ME, Dean JM, Bates FS. Macromolecules 2000;33(7): 2308–10.
[66] Serrano E, Tercjak A, Ocando C, Larrañaga M, Parellada M, Corona-Galvan S, et al. Macromol Chem Phys 2007;208:2281–92.
[67] Argon AS, Cohen RE, Mower TM. Mater Sci Eng A Struct Mater Properties Microstruct Process 1994;176(1–2):79–90.
[68] Pearson RA, Yee AF. J Mater Sci 1986;21(7):2475–88.
[69] Pearson RA, Yee AF. J Mater Sci 1989;24(7):2571–80.
[70] Yang PC, Woo EP, Bishop MT, Pickelman DM, Sue HJ. Polym Mater Sci Eng 1990;63:315–21.
[71] Yee AF, Pearson RA. J Mater Sci 1986;21(7):2462–74.
[72] Garg AC, Mai YW. Compos Sci Technol 1988;31:179–223.
[73] Huang Y, Hunston DL, Kinloch AJ, Riew CK. In: Riew CK, Kinloch AJ, editors. Advances in chemistry series, vol. 233. Washington, DC: American Chemical Society; 1993.
[74] Zhao Q, Hoa SV. J Compos Mater 2007;41(2):201–19.
[75] Kinloch AJ, Shaw SJ, Tod DA, Hunston DL. Polymer 1983;24(4):1355–63.
[76] Sigl LS, Mataga PA, Dageleidish BI, McMeeking RM, Evans AG. Acta Metall 1988;36(4):945–53.
[77] Lange FF. J Mater Sci 1971;54:983–92.
[78] Evans AG, Williams S, Beaumont PWR. J Mater Sci 1985;20:3668–74.
[79] Oritz MJ. Appl Mech 1987;54:54–8.

[80] ASTM-E 399-78. Plane-strain fracture toughness of metallic materials.
[81] Williams JG. Fracture mechanics of polymers. Chichester; 1984.
[82] Ryan AJ, Stanford JL, Still RH. Polymer 1991;32(8):1426–39.
[83] Thio YS, Wu J, Bates FS. Macromolecules 2006;39(21):7187–9.
[84] Berry JP. J Polym Sci 1961;50:107.
[85] Berry JP. In: Liebowitz H, editor. Fracture VII. New York, NY: Academic Press; 1972.
[86] Kelly A. Strong solids. Oxford: Clarendon Press; 1966.
[87] Young RJ. Introduction to polymers. London: Chapman and Hall; 1981.
[88] Wagner HD. Nat Nanotechnol 2007;2:742–4.
[89] Breuer O, Sundararaj U. Polym Compos 2004;25(6):630–45.
[90] Lier GV, Alsenoy CV, Doren VV, Geerlings P. Chem Phys Lett 2000;181–185:326.
[91] Manevitch OL, Rutledge GC. J Phys Chem B 2004;108:1428–35.
[92] Ray SS, Okamoto M. Prog Polym Sci 2003;28:1539–641.
[93] Sturcova A, Davies GR, Eichhorn SJ. Biomolecules 2005;6:1055–61.
[94] Yu M-F, Lourie O, Dyer MJ, Moloni K, Kelly TF, Ruoff RS. Science 2000; 287:637–40.
[95] Samir MASA, Alloin F, Dufresne A. Biomacromolecules 2005;6:612–26.
[96] Jager I, Fratzl P. Biophys J 2000;79:1737–46.
[97] Kamat S, Su X, Ballarini R, Heuer AH. Nature 2000;405:1036–40.
[98] Weiner S, Wagner HD. Annu Rev Mater Sci 1998;28:271–98.
[99] Podsiadlo P, Kaushik K, Arruda EM, Waas AM, Shim S, Xu J, et al. Science 2007;318:80–3.
[100] Jones RAL, Richards RW. Polymers at surfaces and interfaces. Cambridge: Cambridge University Press; 1999.
[101] Angell CA, Ngai KL, McKenna GB, McMillan PF, Martin SW. J Appl Phys 2000;88:3113–57.
[102] Torre R, Bartolini P, Righini R. Nature 2004;428:296–8.
[103] Weeks ER, Crocker JC, Levitt AC, Schofield A, Weitz DA. Science 2000;287:627–31.
[104] Huang Y, Paul DR. Polymer 2004;45:8377–93.
[105] Kurchan J. Nature 2005;433:222–5.
[106] Debenedetti PG, Stillinger FH. Nature 2001;410:259–67.
[107] Silescu HJ. Non-Cryst Solids 1999;243:81–108.
[108] Rabek JF. Experimental methods in polymer science. Chichester: John Wiley; 1980.
[109] Sperling LH. Introduction to physical polymer science. New York, NY: John Wiley; 1986.
[110] Roller MJ. Coat Technol 1982;54(691):33–40.
[111] Starr FW, Schroeder TB, Glotzer SC. Phys Rev E 2001;64:021802–6.
[112] Ellison CJ, Mundra MK, Torkelson JM. Macromolecules 2005;38:1767–78.
[113] Ellison CJ, Tokelson JM. J Polym Sci Part B Polym Phys 2002;40:2745–58.

Gareth Royston earned his undergraduate degree in Chemistry from the University of Sheffield. He stayed at Sheffield to complete his postgraduate research on structured epoxy resin-block copolymer blends under the guidance of Patrick Fairclough. After gaining his Ph.D. in 2007 he moved across the Channel where he is currently a postdoc in the joint CNRS/Rhodia 'Laboratoire Polymères et Matériaux Avancés' in Saint-Fons, France. His present research focuses on the segmental dynamics of polymer blends.
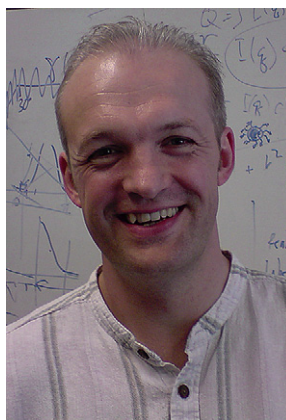
Patrick Fairclough completed his undergraduate degree in Physics at the University of Birmingham. His Ph.D. in Metal Hydrides, under Prof. Keith Ross was also awarded through the University of Birmingham. He then moved to polymeric systems with a postdoctoral position at UMIST, using scattering techniques to characterise the structure of block copolymers with Prof. Tony Ryan and Dr. Colin Booth. He was appointed to the Department of Chemistry at the University of Sheffield in 1997. His current research covers an eclectic mix from salivary proteins to polyolefins.

Lorena Ruiz-Perez completed her undergraduate degree in Physics at the University of Seville. She earned her Ph.D. on interactions between polyelectrolyte networks and brushes within the Polymer Physics Group, in the Department of Physics and Astronomy at the University of Sheffield. Following her Ph.D. in 2006 she worked as a research assistant in the Department of Engineering Materials within the Biomaterials and Tissue Engineering Group. She is currently a postdoctoral research associate with Prof. Tony Ryan in the Department of Chemistry at the University of Sheffield. Her present research involves toughening of thermosets with high number density nanoinclusions.

Tony Ryan has a B.Sc. and a Ph.D. in Polymer Science and Technology from the Victoria University of Manchester and a D.Sc. from UMIST. He is currently the Pro Vice Chancellor for the Faculty of Science at the University of Sheffield. He started his academic career with a lectureship in Polymer Science at UMIST and moved to a Chair in Sheffield where he has been the ICI Professor of Physical Chemistry and Director of the Polymer Centre. His research covers the synthesis, structure, processing and properties of polymers and he is widely engaged in public engagement in science. He presented the Royal Institution Christmas Lectures in 2002 and was made an Officer of the British Empire in 2006.